Journal of Porous Media, 24(6):15–30 (2021)

A NUMERICAL INVESTIGATION OF HALL AND RADIATION EFFECTS ON MHD THREE-DIMENSIONAL CASSON FLUID FLOW IN A POROUS MEDIUM

Prashu,[1] R. Nandkeolyar,[2,*] & Ali J. Chamkha[3]

[1]*School of Mathematics, Thapar Institute of Engineering and Technology, Patiala, Punjab, 147004, India*

[2]*Department of Mathematics, National Institute of Technology Jamshedpur, Jamshedpur, Jharkhand, 831014, India*

[3]*Faculty of Engineering, Kuwait College of Science and Technology, Doha District, Kuwait*

*Address all correspondence to: R. Nandkeolyar, Department of Mathematics, National Institute of Technology Jamshedpur, Jamshedpur, Jharkhand, 831014, India, E-mail: rajnandkeolyar@gmail.com

Original Manuscript Submitted: 3/13/2018; Final Draft Received: 11/21/2018

This work presents a numerical analysis of the time-dependent three-dimensional hydromagnetic Casson fluid flow along a stretching surface through a porous medium considering the effects of Hall current and nonlinear radiation. The mathematical model of the problem is presented in the form of a set of nonlinear partial differential equations along with suitable boundary conditions. These equations are transformed to a set of nonlinear ordinary differential equations using suitable similarity transformations which are later dealt with the efficient spectral quasi-linearization method (SQLM) to obtain the numerical solution of the considered model. A parametric study involving the emerging physical parameters is performed to analyze the effects of relevant flow parameters on the fluid velocity, fluid temperature, and coefficients of skin-friction and heat transfer at the surface. It is found that the momentum boundary layers, in both directions, get thicker whereas the thermal boundary layer becomes thinner with increasing Hall current.

KEY WORDS: *Casson fluid, convecting heating, Hall current, Rosseland approximation, porous medium*

1. INTRODUCTION

Boundary layer flow of a viscous fluid finds applications in many engineering processes, such as in paper production, glass production, and steel production. In steel production, a better outcome in the manufacturing process is achieved by controlling the cooling rate of the liquid and the stretching rate of the sheet. The rapid stretching of the sheet may finally affect the penultimate quality of the product. As a result, the theoretical study of the flow of a viscous fluid over a stretching surface was investigated by several researchers. The study of laminar boundary layer flow of viscous fluid along a stretching surface was pioneered by Crane (1970). Following the study of Crane (1970) several researchers (Elbashbeshy, 1998; Mahapatra and Gupta, 2002; Patil et al., 2010) investigated the flow of a viscous fluid over a stretching surface considering different aspects of the problem and under different geometrical conditions. It is well known that the implication of presence of a magnetic field in the flow of a viscous incompressible electrically conducting fluid results in the production of a resistive force in the flow field which acts as a stabilizing agent to the flow and delays the boundary layer separation. The boundary layer flow of a viscous and electrically conducting fluid in the presence of a magnetic field is encountered in several engineering devices, such as in geothermal heat pumps, MHD generators, MHD flow meters, and MHD propulsion systems. In heat transfer processes, the desired properties of the final product can be obtained by controlling the rate of cooling. In order to control the cooling rate,

NOMENCLATURE

a	a constant
A	unsteadiness parameter
$B(t)$	time-dependent magnetic field
C	convective heating parameter
C_{fx}	skin-friction coefficient in x-direction
C_{fz}	skin-friction coefficient in z-direction
c_p	specific heat capacity at constant pressure
f', g	dimensionless velocities in x- and z-directions
h_s	convective heat transfer coefficient
k	thermal conductivity of the fluid
K	permeability of the porous medium
m	Hall current parameter
M	magnetic parameter
N_r	radiation parameter
Nu_x	local Nusselt number
Pr	Prandtl number
q_w	wall heat transfer coefficient
Re_x	local Reynolds number
T	temperature of the fluid
t	time variable
T_∞	fluid temperature at infinity
T_w	fluid temperature at the surface
tr	temperature ratio parameter
$u_w(x,t)$	time dependent stretching velocity
u, v, w	velocity components in x-, y-, and z-directions
x, y, z	space variables

Greek Symbols

α^*	Rosseland mean absorption coefficient
α_m	thermal diffusivity of the fluid
β	Casson fluid parameter
η	similarity variable
γ	a constant
λ	permeability parameter
μ	coefficient of viscosity of the fluid
μ_e	effective viscosity of the fluid
ν	kinematic coefficient of viscosity
ρ	density of the fluid
σ	electrical conductivity of the fluid
σ^*	Stefan–Boltzmann constant
τ_{wx}	shear-stress component in x-direction
τ_{wz}	shear-stress component in z-direction
θ	dimensionless fluid temperature

the flow field is also subjected to an externally applied magnetic field. For these reasons, the magnetohydrodynamic flow of a viscous fluid was studied by several researchers. The study of MHD fluid flow toward a stretching sheet was introduced by Pavlov (1974) who first extended the idea of Crane (1970) including the effects of an applied magnetic field. Kumaran et al. (2009) examined the MHD boundary layer fluid flow to obtain the analytical solution along with a quadratically stretching sheet. Rashidi et al. (2013) analyzed the second law of thermodynamics on the magnetohydrodynamic boundary layer flow of a nanofluid over a rotating porous disk. Nandkeolyar et al. (2014, 2013) investigated the homogeneous and heterogeneous reaction effects on the flow of a viscous nanofluid along the stretching sheet in the presence of an external magnetic field under different conditions. Sheikholeslami et al. (2016) considered the effects of a variable magnetic field on the forced convection heat transfer in a ferrofluid filled semi-annulus lid.

When the strength of the externally applied magnetic field is strong and/or the density of the electrically conducting working fluid is low, the effect of Hall current becomes significant, which induces a flow in the secondary direction. Even though, the Hall effect phenomenon was discovered by Edwin Herbert Hall in 1879, it took several years for the researchers to feel the impetus toward the study of Hall current effects on hydromagnetic flows. Gupta (1975) was perhaps the first to investigate the influence of Hall current on the magnetohydrodynamic fluid flow along a porous surface. Reddy and Bathaiah (1982) discussed the problem involving the effects of Hall current on the steady flow of a viscous incompressible and electrically conducting fluid in the presence of a magnetic field. Saleem and Aziz (2008) studied the combined influence of Hall current and mass diffusion on laminar flow of a hydromagnetic heat generating/absorbing fluid. Seth et al. (2010) considered the effects of Hall current on the Hartmann flow of a viscous and incompressible fluid under the influence of an inclined magnetic field. Sarkar et al. (2014) further investigated the effects of Hall current on the hydromagnetic rotating flow of an electrically conducting fluid within a parallel plate channel. The influence of Hall current on the hydromagnetic boundary layer flow of an electrically conducting fluid over a variable thickness stretching sheet was investigated by Prasad et al. (2016). It was observed by Prasad et al. (2016) that the presence of Hall current has a significant effect on the flow and heat transfer within the boundary layer region and the Hall current induces a cross flow in the flow field. These investigations mostly deal with the steady-state aspect of the problem and assume the fluid properties to be independent of time. However, to study the flow characteristics of real-life problems, it is essential to investigate the models that are transient. Wang (1990) made the first attempt to analyze the unsteady-state fluid flow problem using a particular type of similarity transformation which transformed the governing partial differential equations into ordinary differential equations in similar form. Elbashbeshy and Bazid (2004) examined the heat transfer characteristics of the hydromagnetic flow of a viscous fluid toward a time-dependent stretching surface. They inferred a decrease in the thickness of both the momentum and thermal boundary layers with increasing unsteadiness in the flow field. Ishak et al. (2009) studied the heat transfer properties of the unsteady boundary layer flow problem over a vertical stretching surface. Chamkha (1997) studied the influence of Hall current on the hydromagnetic natural convective flow of viscous and electrically conducting fluid flow in a stratified porous medium. The implications of Hall current in a rotating flow of a second-grade fluid toward a stretching surface in a porous medium was studied by Hayat et al. (2008). Saleem and Aziz (2008) presented a study to investigate the simultaneous influence of Hall current and mass diffusion on laminar flow of a hydromagnetic heat generating/absorbing fluid. Hussain et al. (2017) made an attempt to examine the effects of Hall current and heat absorption on the natural convection flow induced due to an accelerated plate in the presence of chemical reaction.

The effect of radiative heat transfer on the flow of a viscous incompressible fluid appears due to the presence of temperature differences between the surrounding and the ambient fluid. Radiative heat transfer also affects the penultimate product that is to be produced. Several authors have considered the influence of radiative heat transfer effects on the boundary layer flow of a Newtonian fluid under different conditions. Aziz (2009) obtained the similarity solutions for the unsteady boundary layer flow in the presence of a radiative heat transfer. The combined effects of Hall current and radiative heat transfer for the time-dependent hydromagnetic fluid flow along a porous surface was analyzed by Pal (2013). Ram et al. (2013, 2017) and Singh et al. (2014) have extensively studied the problems related to unsteady heat and mass transfer in MHD radiating/reacting fluids flow past a moving vertical porous plate in the presence of source/sink. In these studies, authors have considered an ordinary viscous fluid under the influence of uniform transverse/cosinusoidal magnetic field. Seth et al. (2015, 2016) obtained the exact results of the Hall effects on the transient hydromagnetic natural convective heat and mass transfer flow in a porous medium including effects of heat absorption and thermal radiation. In these studies, the authors also included the influence of the Coriolis force. It was found in the study of Seth et al. (2016) that the rate of heat transfer is increased with increasing heat absorption and thermal radiation, whereas the Hall current reduced the primary shear stress and increased the shear stress in the secondary direction.

The study of the magnetohydrodynamic flow of a Newtonian fluid through a porous medium has attracted the attention of many researchers due to its applications in the optimization of solidification processes of metals and metal alloys. Rashad et al. (2014) presented a numerical simulation to discuss the effect of thermal radiation, permeability of the medium, and chemical reaction on the flow of a viscous fluid in a square enclosure. The steady mixed convective boundary layer flow of a viscous nanofluid about a solid sphere with convective heating at the surface in the presence of thermal radiation and Darcy porous medium was investigated by El-Kabeir et al. (2015). Nabwey et al. (2015) presented Lie group analysis to study the implications of thermal radiation, chemical reaction, and velocity slip on the unsteady heat and mass transfer in a laminar flow of a viscous and incompressible fluid along a horizontal stretching surface embedded in porous medium. Mallikarjuna et al. (2016) investigated the effects of thermal radiation and transpiration on the flow and heat transfer in a non-Darcy convective flow of a viscous fluid flow adjacent to a rotating vertical cone. Joshi et al. (2017, 2018) have also carried numerical investigations about porosity effects of magnetic nanofluids over a moving/stationary stretchable disk. Some recent contributions on the magnetohydrodynamic flow of a Newtonian fluid in a porous medium under different conditions are also due to Makinde et al. (2018), Sekhar et al. (2018), and Sheikholeslami and Abelman (2018).

Unlike the Newtonian fluids, the rheological properties of non-Newtonian fluids cannot be described by a single model, and hence researchers have developed different models to study the flow behavior of different types of non-Newtonian fluids. One such type of non-Newtonian fluid model is the Casson fluid model, which is based on the yield stresses. The Casson fluid model includes the interaction of solid and liquid phases. When the yield stresses are more significant than shear stresses, the Casson fluid acts like a solid. On the other hand, when yield stresses are less than the shear stresses, the fluid starts moving. Examples of liquids following the Casson fluid model in our day-to-day life are chilly sauce, honey, jelly, and condensed milk. The Casson fluid model also finds applications in drug delivery during cancer therapy as the flow of blood within the artery can be treated as a Casson fluid flow. Keeping in view the important applications of this model, several researchers investigated the flow and heat transfer properties in a Casson fluid flow. Eldabe and Salwa (1995) were the first to study the Casson fluid flow between two coaxial cylinders. However, it took many years before many researchers conducted the theoretical study of Casson fluid flow under different conditions and configurations. Shehzad et al. (2013) examined the heat and mass transfer in hydromagnetic non-Newtonian liquid flow by considering the chemical reaction and suction effects. Tufail et al. (2013) analyzed the heat source/sink impacts on magnetohydrodynamic fluid flow and heat transfer toward a porous stretching surface. The partial velocity-slip effects in MHD Casson liquid flow along a stretching surface are investigated by Nandy (2013). He obtained the solutions which are analytic about the stagnation point. Mukhopadhyay (2013) studied the heat transfer phenomenon in MHD Casson liquid flow along a stretching sheet. Vajravelu et al. (2013) studied the flow and heat transfer of a Casson liquid due to an exponentially stretching permeable surface. Mukhopadhyay and Vajravelu (2013) examined the unsteady-state problem for Casson liquid toward a porous surface. Ashraf et al. (2017) investigated the mixed convection flow of a Casson liquid in the presence of Hall effect along a stretching surface. Butt et al. (2016) investigated the time-dependent three-dimensional flow of an electrically conducting fluid embedded into the porous medium in the presence of a magnetic field. The mixed convective boundary layer Casson fluid flow about a solid sphere including the effects of chemical reaction was studied by El-Kabeir et al. (2016). In this study, the authors also included the hydrodynamic, thermal, and solutal slip effects and solved the resulting model numerically using finite difference technique. Khan et al. (2017) investigated the homogeneous-heterogeneous reactions for Casson liquid flow.

To the best of the authors' knowledge, no one has studied the simultaneous effects of Hall current and nonlinear Rosseland thermal radiation on the transient three-dimensional flow of a viscous and incompressible Casson fluid in a fluid saturated porous medium along a convectively heated stretching surface. Keeping this in mind, our aim through this article is to numerically investigate a time-dependent model for the three-dimensional hydromagnetic Casson fluid flow along a stretching surface embedded in a porous medium considering the combined effects of Hall current, nonlinear radiation, and convective heating at the surface. The mathematical model describing the physics of the problem is in the form of a set of nonlinear partial differential equations along with suitable boundary conditions. The governing nonlinear partial differential equations are reduced to a set of nonlinear ordinary differential equations using a suitable similarity transformation. To obtain the numerical solutions of the nondimensionalized coupled nonlinear differential equations, an efficient technique, namely the spectral quasi-linearization method, is employed. The effects of several parameters on the flow and heat transfer characteristics are studied with the help of suitable graphs and tables.

2. THE MATHEMATICAL MODEL

Let us consider a transient three-dimensional flow of a Casson fluid along a convectively heated stretching sheet embedded in a fluid-saturated porous medium under the influence of an applied magnetic field.

The stretching surface is assumed to be in the plane $y = 0$, and the Casson fluid is confined in the region $y \geq 0$. The fluid flow in the region $y \geq 0$ is induced due the linear stretching of the sheet along the x-axis with a velocity $u = u_w(x, t)$. The fluid flow is permeated with an externally applied magnetic field $B(t)$ acting in the y-direction. In addition to these, the following assumptions are made:

1. The density of the fluid is low and/or the strength of the magnetic field is high so that the effects of Hall current become significant.

2. The magnetic Reynolds number of the fluid is small in comparison to the applied one so that the effect of induced magnetic field is neglected.

3. The fluid is optically thick, and a nonlinear Rosseland diffusion approximation is employed to study the effects of radiative heat transfer.
4. The Casson fluid is flowing in a saturated porous medium.

Under the preceding assumptions, and using the Rosseland approximation, the equations governing the flow and heat transfer in the unsteady three-dimensional magnetohydrodynamic flow of a Casson fluid along a stretching sheet within a fluid-saturated porous medium in the presence of Hall current, and nonlinear radiative heat transfer, are

$$\frac{\partial u}{\partial x}+\frac{\partial v}{\partial y}+\frac{\partial w}{\partial z}=0, \tag{1}$$

$$\frac{\partial u}{\partial t}+u\frac{\partial u}{\partial x}+v\frac{\partial u}{\partial y}+w\frac{\partial u}{\partial z}=\nu\left(1+\frac{1}{\beta}\right)\frac{\partial^2 u}{\partial y^2}-\frac{\sigma B^2(t)}{\rho(1+m^2)}(u+mw)-\frac{\mu_e}{\rho K}u, \tag{2}$$

$$\frac{\partial w}{\partial t}+u\frac{\partial w}{\partial x}+v\frac{\partial w}{\partial y}+w\frac{\partial w}{\partial z}=\nu\left(1+\frac{1}{\beta}\right)\frac{\partial^2 w}{\partial y^2}+\frac{\sigma B^2(t)}{\rho(1+m^2)}(mu-w)-\frac{\mu_e}{\rho K}w, \tag{3}$$

$$\frac{\partial T}{\partial t}+u\frac{\partial T}{\partial x}+v\frac{\partial T}{\partial y}+w\frac{\partial T}{\partial z}=\frac{\partial}{\partial y}\left[\left(\alpha_m+\frac{16\sigma^* T^3}{3\alpha^*\rho c_p}\right)\frac{\partial T}{\partial y}\right], \tag{4}$$

where the components of velocity in the x-, y-, and z-directions are represented as u, v, and w, respectively; t is taken as time; β is the Casson liquid parameter; μ_e denotes the effective viscosity of the fluid; K is the permeability of the porous medium; σ is electrical conductivity of the fluid; ρ is density of the fluid; $\nu=\mu/\rho$ is the liquid's kinematic viscosity; m is Hall current parameter; $\alpha_m=k/(\rho c_p)$ represents the liquid's thermal diffusivity. The Stefan–Boltzmann constant and coefficient of Rosseland mean absorption are denoted as σ^* and α^*, respectively; c_p is specific heat capacitance at constant pressure; and T is the temperature within the boundary layer.

The appropriate boundary conditions for the physical problem are

$$\text{At } y=0:\ \ u=u_w,\ \ v=0,\ \ w=0,\ \ \frac{\partial T}{\partial y}=-h_s T; \tag{5}$$

$$\text{As } y\to\infty:\ \ u\to 0,\ \ w\to 0,\ \ T\to T_\infty, \tag{6}$$

where h_s is the convective heat transfer coefficient. In the present problem the stretching velocity is assumed as $u_w(x,t)=(ax)/(1-\gamma t)$ and the time-dependent magnetic field is taken as $B(t)=B_0(1-\gamma t)^{-1/2}$, where a and γ are constants and B_0 is the strength of the magnetic field.

We now choose a transformation of the form

$$u=\frac{ax}{(1-\gamma t)}f'(\eta),\ \ v=-\sqrt{\frac{a\nu}{(1-\gamma t)}}f(\eta),\ \ w=\frac{ax}{(1-\gamma t)}g(\eta), \tag{7}$$

$$\theta(\eta)=\frac{T-T_\infty}{T_\infty},\ \ \eta=y\sqrt{\frac{a}{\nu(1-\gamma t)}}, \tag{8}$$

so that the equation of continuity Eq. (1) is automatically satisfied and the Eqs. (2)–(4) reduce to

$$\left(1+\frac{1}{\beta}\right)f'''+ff''-(f')^2-A\left(f'+\frac{\eta}{2}f''\right)-\frac{M}{(1+m^2)}(f'+mg)-\lambda f'=0, \tag{9}$$

$$\left(1+\frac{1}{\beta}\right)g''-gf'+fg'-A\left(g+\frac{\eta}{2}g'\right)+\frac{M}{(1+m^2)}(mf'-g)-\lambda g=0, \tag{10}$$

$$\left(1+\frac{4}{3N_r}(1+\theta)^3\right)\theta''-\Pr A\frac{\eta}{2}\theta'+\Pr f\theta'+\frac{4}{N_r}(1+\theta)^2\theta'^2=0. \tag{11}$$

The boundary conditions in Eqs. (7) and (8) reduce to

$$\text{At } \eta=0:\quad f'=1,\quad f=0,\quad g=0,\quad \theta'=-C(1+\theta); \tag{12}$$

$$\text{As } \eta\to\infty:\quad f'\to 0,\quad g\to 0,\quad \theta\to 0, \tag{13}$$

where η is the dimensionless similarity variable and the primes denote derivative with respect to η. The nondimensional parameters used previously are defined as

$$A = \frac{\gamma}{a}, \quad M = \frac{\sigma B_0^2}{\rho a}, \quad N_r = \frac{k\alpha^*}{4\sigma^* T_\infty^3}, \quad \text{Pr} = \frac{\nu}{\alpha_m}, \quad \lambda = \frac{\mu_e}{\rho K}\frac{\text{Re}_x}{\text{Re}_k^2}, \quad C = -h_s\sqrt{\frac{\nu(1-ct)}{a}},$$

where A, M, N_r, Pr, λ, and C are, respectively, the unsteadiness parameter, magnetic field parameter, radiation parameter, Prandtl number, local porosity parameter, and the convective heating parameter.

Apart from the velocity and temperature fields, the important physical quantities of engineering interest are the friction coefficients along x- and z-directions, and the local Nusselt number. These are denoted in the text as C_{fx}, C_{fz}, and Nu_x, respectively, and are defined as

$$C_{fx} = \frac{\tau_{wx}}{\rho u_w^2}, \quad C_{fz} = \frac{\tau_{wz}}{\rho u_w^2}, \quad \text{Nu}_x = \frac{xq_w}{k(T - T_\infty)}, \tag{14}$$

where the shear-stress components τ_{wx}, τ_{wz}, and the rate of heat transfer at the surface q_w, are defined as

$$\tau_{wx} = \mu\left(1+\frac{1}{\beta}\right)\left(\frac{\partial u}{\partial y}\right)_{y=0}, \quad \tau_{wz} = \mu\left(1+\frac{1}{\beta}\right)\left(\frac{\partial w}{\partial y}\right)_{y=0}, \quad q_w = \left[-k\left(\frac{\partial T}{\partial y}\right) + q_r\right]_{y=0}. \tag{15}$$

Therefore, the values of C_{fx}, C_{fz}, and Nu_x, respectively, are given by

$$C_{fx}\text{Re}_x^{1/2} = \left(1+\frac{1}{\beta}\right)f''(0), \quad C_{fz}\text{Re}_x^{1/2} = \left(1+\frac{1}{\beta}\right)g'(0); \tag{16}$$

$$\text{Re}_x^{-1/2}\text{Nu}_x = C\left[1 + \frac{4}{3N_r}(1+\theta(0))^3\right]\left(1+\frac{1}{\theta(0)}\right), \tag{17}$$

where q_r is the radiative heat flux and $\text{Re}_x = (xu_w)/\nu$ is the local Reynolds number.

3. NUMERICAL SOLUTION

The governing nondimensionalized nonlinear ordinary differential equations in Eqs. (9)–(11) are solved using an efficient numerical technique known as spectral quasi-linearization method (SQLM). SQLM follows the idea of linearizing the nonlinear differential equations using linear Taylor series approximation. In the framework of SQLM, we obtain the linearized iteration scheme as

$$a_{11}^{(3)}f_{r+1}''' + a_{11}^{(2)}f_{r+1}'' + a_{11}^{(1)}f_{r+1}' + a_{11}^{(0)}f_{r+1} + a_{12}^{(0)}g_{r+1} = R_1, \tag{18}$$

$$a_{22}^{(2)}g_{r+1}'' + a_{22}^{(1)}g_{r+1}' + a_{22}^{(0)}g_{r+1} + a_{21}^{(1)}f_{r+1}' + a_{21}^{(0)}f_{r+1} = R_2, \tag{19}$$

$$a_{33}^{(2)}\theta_{r+1}'' + a_{33}^{(1)}\theta_{r+1}' + a_{33}^{(0)}\theta_{r+1} + a_{31}^{(0)}f_{r+1} = R_3, \tag{20}$$

where

$$a_{11}^{(3)} = \left(1+\frac{1}{\beta}\right), \ a_{11}^{(2)} = f_r - A\frac{\eta}{2}, \ a_{11}^{(1)} = -2f_r' - A - \frac{M}{1+m^2} - \lambda, \ a_{11}^{(0)} = f_r'', \ a_{12}^{(0)} = -\frac{Mm}{1+m^2},$$

$$R_1 = f_r f_r'' - (f_r')^2, \ a_{22}^{(2)} = \left(1+\frac{1}{\beta}\right), \ a_{22}^{(1)} = f_r - A\frac{\eta}{2}, \ a_{22}^{(0)} = -f_r' - A - \frac{M}{1+m^2} - \lambda,$$

$$a_{21}^{(1)} = -g_r + \frac{Mm}{1+m^2}, \ a_{21}^{(0)} = g_r', \ R_2 = -g_r f_r' + g_r' f_r, \ a_{33}^{(2)} = \frac{4}{3N_r}(1+\theta_r)^3 + 1,$$

$$a_{33}^{(1)} = -A\text{Pr}\frac{\eta}{2} + \text{Pr}f_r + \frac{8}{N_r}(1+\theta_r)^2\theta_r', \ a_{33}^{(0)} = \frac{4}{N_r}(1+\theta_r)^2\theta_r'' + \frac{8}{N_r}(1+\theta_r)(\theta_r')^2,$$

$$R_3 = \frac{N_r\text{Pr}\,f_r\theta_r' + 4(1+\theta_r)(\theta_r(1+\theta_r)\theta_r'' + (3\theta_r+1)(\theta_r')^2)}{N_r}.$$

The corresponding boundary conditions for the iteration scheme are

$$\text{At } \eta = 0: \quad f'_{r+1} = 1, \quad f_{r+1} = 0, \quad g_{r+1} = 0, \quad \theta'_{r+1} = -C(1 + \theta_{r+1}), \tag{21}$$

$$\text{As } \eta \to \infty: \quad f'_{r+1} \to 0, \quad g_{r+1} \to 0, \quad \theta_{r+1} \to 0. \tag{22}$$

The preceding iteration scheme requires initial approximations to start with, which are chosen to be convenient functions satisfying the boundary conditions as

$$f_0 = 1 - e^{-\eta}, \quad h_0 = 0, \quad \theta_0 = \left(\frac{C}{1 - C}\right) e^{-\eta}.$$

The Chebyshev pseudo-spectral collocation method is used to solve the linearized Eqs. (18)–(20). The domain of the physical problem $[0,\ \infty)$ is approximated with $[0,\ L]$, where L is used to invoke the boundary conditions at ∞. The computational domain $[0,\ L]$ is then transformed to $[-1,\ 1]$ by using the transformation $\eta = L(\xi + 1)/2$ so that the Gauss–Lobatto points can be used to discretize the computational domain. The derivatives of the unknown functions at the grid points, in the linearized equations, are approximated with the Chebyshev differentiation matrix. The application of the Chebyshev pseudo-spectral collocation method yield us

$$\begin{pmatrix} A_{11} & A_{12} & A_{13} \\ A_{21} & A_{22} & A_{23} \\ A_{31} & A_{32} & A_{33} \end{pmatrix} \begin{pmatrix} f_{r+1} \\ g_{r+1} \\ \theta_{r+1} \end{pmatrix} = \begin{pmatrix} R_1 \\ R_2 \\ R_3 \end{pmatrix},$$

where each A_{ij} is of order $(N + 1) \times (N + 1)$. f_{r+1}, g_{r+1}, θ_{r+1}, R_1, R_2, and R_3 are vectors of order $(N + 1) \times 1$.

4. RESULTS AND DISCUSSION

The present article numerically investigates the flow and heat transfer characteristics due to the unsteady three-dimensional hydromagnetic flow of a Casson fluid along a stretching sheet in a fluid-saturated porous medium. The primary purpose of the work is to highlight the combined effects of Hall current, the porosity of the medium, nonlinear thermal radiation, and convective heating of the surface on the fluid flow and heat transfer. In an attempt to fulfill the primary objective, suitable similarity transformations are used to reduce the governing nonlinear partial differential equations to a set of coupled nonlinear ordinary differential equations. Several pertinent nondimensional parameters appear in the nonlinear coupled ordinary differential equations, such as magnetic parameter M, Hall current parameter m, Casson fluid parameter β, porosity parameter λ, unsteadiness parameter A, Prandtl number Pr, and convective parameter C. To investigate the effect of these parameters, Eqs. (9)–(11) are solved using SQLM, and the profiles of fluid velocities $f'(\eta)$ and $g(\eta)$, and fluid temperature $\theta(\eta)$ are presented in Figs. 1–5. The numerical values of coefficients of skin friction C_{fx}, C_{fz}, and coefficient of heat transfer, formally known as Nusselt number Nu_x, are tabulated in Table 1.

Figure 1 presents the effect of the magnetic parameter M and the Hall current parameter m on the fluid velocity in the x-direction $f'(\eta)$, fluid velocity in the z-direction $g(\eta)$, and the fluid temperature $\theta(\eta)$ within the boundary layer region. The magnetic parameter M measures the strength of the Lorentz force that appears in the flow field due to the presence of the external magnetic field while the Hall current parameter m measures effect of Hall current, which appears in the flow field due to the presence of a strong magnetic field and/or if the density of the fluid is low. Figure 1 shows that the Lorentz force appearing due to the magnetic field acts as a resistive force in the flow field, and it decelerates the fluid flow in the x-direction throughout the boundary layer region. The fluid flow in z-direction gets accelerated but only in a region near to the stretching surface, whereas it gets decelerated afterward before attaining the free-stream velocity. The implication of the Hall current in the flow field is to accelerate the fluid velocities in both directions. However, the noted impact is significant on the fluid velocity in the z-direction. The magnetic field generated Lorentz force and the Hall current have opposite effects on the fluid temperature. The fluid temperature is found to be an increasing function of the magnetic field parameter but a decreasing function of the Hall current parameter.

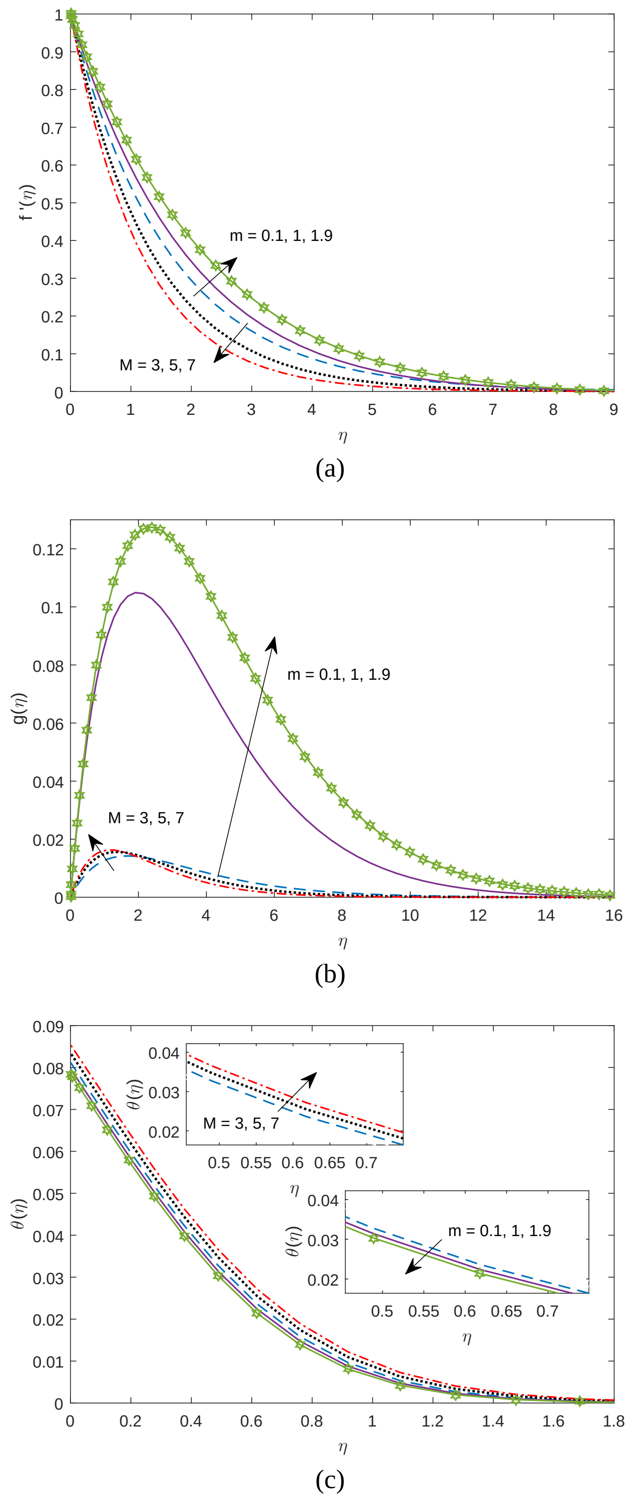

FIG. 1: Effect of magnetic parameter M and Hall current parameter m on (a) f', (b) g, and (c) θ when $A = 0.1$, $\lambda = 0.1$, $\beta = 0.1$, $N_r = 1$, $\Pr = 10$, and $C = 0.1$

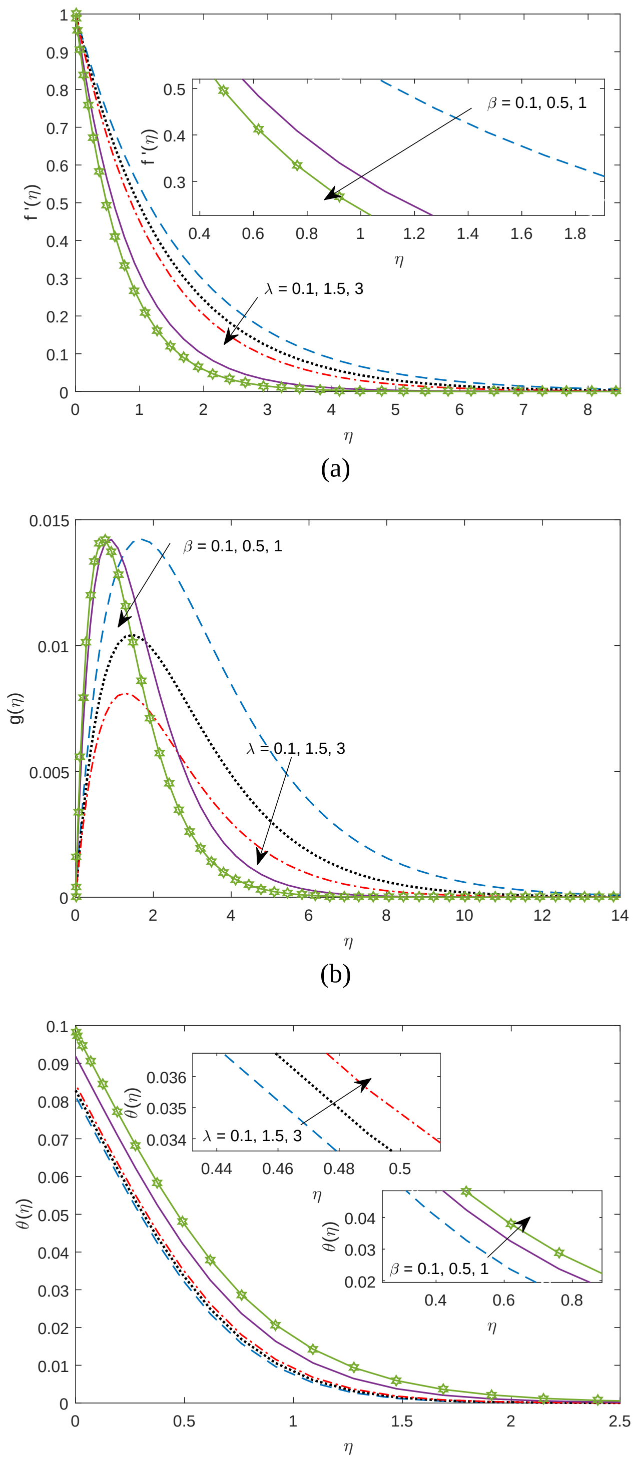

FIG. 2: Effect of Casson parameter β and porosity parameter λ on (a) f', (b) g, and (c) θ when $A = 0.1$, $m = 0.1$, $M = 3$, $N_r = 1$, $\Pr = 10$, and $C = 0.1$

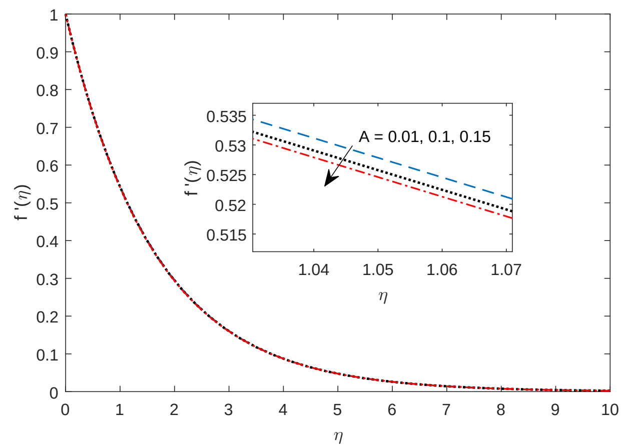

(a)

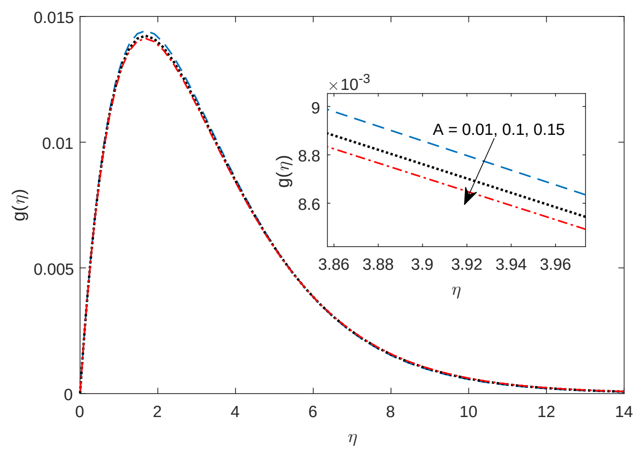

(b)

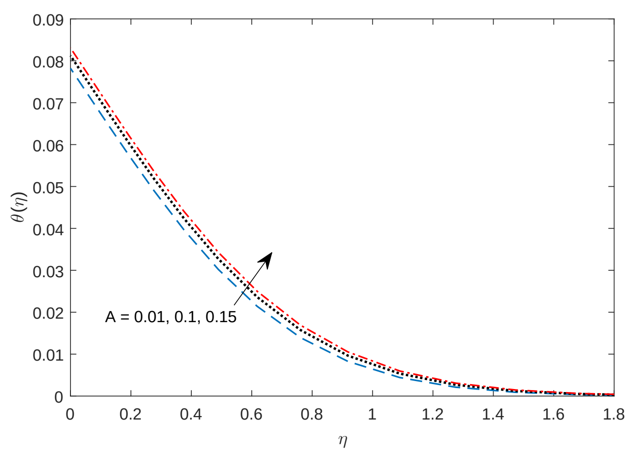

(c)

FIG. 3: Effect of unsteadiness parameter A on (a) f', (b) g, and (c) θ when $m = 0.1$, $\lambda = 0.1$, $\beta = 0.1$, $N_r = 1$, Pr $= 10$, and $M = 3$

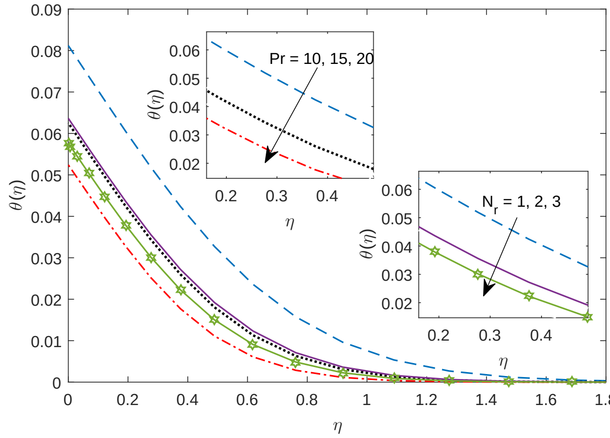

FIG. 4: Effect of radiation parameter N_r and Prandtl number Pr on θ when $m = 0.1$, $\lambda = 0.1$, $\beta = 0.1$, $A = 0.1$, $C = 0.1$, and $M = 3$

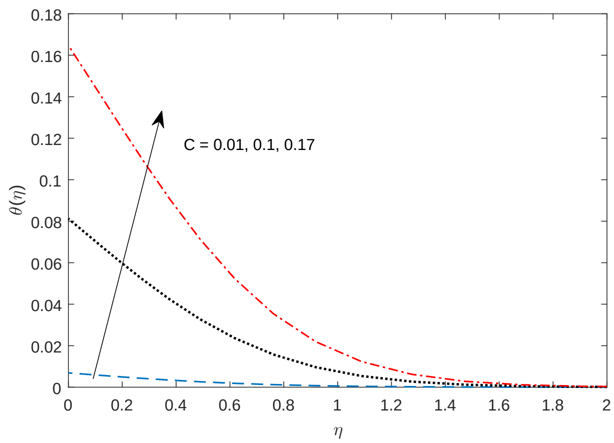

FIG. 5: Effect of convective parameter C on θ when $m = 0.1$, $\lambda = 0.1$, $\beta = 0.1$, $A = 0.1$, $\Pr = 10$, $N_r = 1$, and $M = 3$

The influence of Casson fluid parameter β and the porosity parameter λ on the fluid velocities in x- and z-directions, and on the fluid temperature is shown in Fig. 2. One must note that the Casson parameter β measures the yield stress and the fluid behaves as a Newtonian fluid as $\beta \to \infty$. Also, the porosity parameter λ is inversely proportional to the permeability of the medium, i.e., smaller the value of λ the higher is the permeability of the medium. It resembles from the figure that the fluid velocities in x- and z-directions decrease with increasing values of λ, and this shows that these velocities are higher in mediums with higher permeability. The fluid velocity in x-direction decreases with increasing Casson parameter β. Therefore, it follows that the fluid velocity in a Casson fluid is higher than that of a Newtonian fluid. The fluid velocity in the z-direction also follows this trend except for increasing near the surface of the stretching sheet with an increase in the Casson parameter β. The fluid temperature, within the boundary layer region, rises with an increase in either λ or β, which implies that the temperature of the fluid is higher in the case of a Newtonian fluid and lesser in a medium with higher permeability.

The unsteadiness parameter A measures the transient behavior of the flow and heat transfer and the flow field becomes steady when $A = 0$. Figure 3 captures the implications of increasing unsteadiness parameters on the fluid velocity in the x-direction $f'(\eta)$, fluid velocity in the z-direction $g(\eta)$, and fluid temperature $\theta(\eta)$. From the observed results, it is clear that the fluid velocity in both the directions gets decelerated with increasing unsteadiness in the flow

TABLE 1: Influence of different parameters on skin-friction coefficients and Nusselt number

M	m	A	N_r	C	β	Pr	λ	$-C_{fx}\mathrm{Re}_x^{1/2}$	$C_{fz}\mathrm{Re}_x^{1/2}$	$\mathrm{Re}_x^{-1/2}\mathrm{Nu}_x$
3	0.1	0.1	1	0.1	0.1	10	0.1	6.75668869	0.25242903	3.57521555
5								8.21533482	0.34099012	3.50034797
7								9.45142273	0.41197207	3.43616354
	0.1							6.75668869	0.25242903	3.57521555
	1							5.65134497	1.55455540	3.62835138
	1.9							4.76295267	1.56554520	3.67298301
		0.01						6.70234056	0.25460189	3.68312501
		0.1						6.75668869	0.25242903	3.57521555
		0.15						6.78675232	0.25123802	3.51317283
			1					6.75668869	0.25242903	3.57521555
			2					6.75668869	0.25242903	3.01147937
			3					6.75668869	0.25242903	2.79957595
				0.01				6.75668869	0.25242903	3.44113263
				0.1				6.75668869	0.25242903	3.57521555
				0.17				6.75668869	0.25242903	3.73455556
					0.1			6.75668869	0.25242903	3.57521555
					0.5			3.52856559	0.13182676	3.25256053
					1			2.88106174	0.10763610	3.09495642
						10		6.75668869	0.25242903	3.57521555
						15		6.75668869	0.25242903	4.41622642
						20		6.75668869	0.25242903	5.12636593
							0.1	6.75668869	0.25242903	3.57521555
							1.5	7.81266622	0.21582339	3.52117747
							3	8.80504026	0.19016116	3.46994702

field whereas the fluid temperature experiences a rise in case of a transient flow. These effects on the fluid velocities and heat transfer, however, are not that significant.

Figure 4 captures the variations in fluid temperature $\theta(\eta)$ with increasing values of N_r and Pr. The radiation parameter N_r measures the effect of radiative heat transfer on the fluid temperature and is inversely proportional to the radiation effect. Therefore, increasing values of N_r correspond to decreasing radiative heat transfer effect and vice versa. From this figure, one may note that the fluid temperature $\theta(\eta)$ falls with increasing values of N_r, which shows that the radiative heat transfer tends to increase the fluid temperature within the boundary layer region. The radiation contributes to the thermal energy of the system, which forces the fluid temperature to rise in the flow field. The Prandtl number Pr is the ratio of viscous diffusivity to thermal diffusivity, and an increase in Prandtl number leads to a decrease in the thermal diffusivity of the fluid. Figure 4 shows that the fluid temperature is a decreasing function of the Prandtl number of the fluid, which implies that the increasing thermal diffusivity leads to higher fluid temperature. The convective heating parameter C signifies the impact of convective heating at the surface. Behavior of fluid temperature with increasing values of the convective parameter is presented in Fig. 5, and it follows that the temperature of the fluid, within the boundary layer region, rises with the increase in the convective heating at the surface. This increase in temperature happens as a result of heat transfer that takes place from the surface to the fluid lying in the boundary layer region.

The effects of pertinent flow parameters, viz. the magnetic parameter M, Hall current parameter m, unsteadiness parameter A, Casson fluid parameter β, and porosity parameter λ on the skin-friction coefficients C_{fx} and C_{fz}, and on the coefficient of heat transfer at the surface Nu_x, is presented in Table 1. The coefficient of skin friction in the x-direction C_{fx} increases with increasing values of the magnetic parameter, unsteadiness parameter, and porosity parameter, whereas it decreases upon increasing the Hall current parameter and the Casson fluid parameter. Thus, the skin-friction coefficient in the x-direction increases with the increasing strength of the Lorentz force and the unsteadiness in the flow field, whereas the Hall current tends to reduce it. A Newtonian fluid has lesser skin-friction coefficient C_{fx} as compared to a Casson fluid. The skin-friction coefficient is higher in the case of a lesser permeable medium. It follows from Table 1 that the skin-friction coefficient in the z-direction C_{fz} increases with increasing effects of the Lorentz force, Hall current, and the permeability of the medium, while it decreases with the increase in the unsteadiness in the flow field. The coefficient of heat transfer at the surface Nu_x decreases with increase in the strength of the magnetic field, unsteadiness, Casson parameter, and permeability of the medium, whereas it increases with the increase in the Hall current. Since the heat transfer coefficient decreases with increasing values of the Casson parameter, it follows that the heat transfer from the surface is higher in the case of Casson liquids than in the case the Newtonian fluids. Table 1 also reflects the influence of the radiation parameter N_r, convective heating parameter C, and the Prandtl number Pr. Following the tabulated values, it is clear that the heat transfer at the surface increases with increasing values of the thermal radiation, convective heating, and Prandtl number.

5. CONCLUSIONS

The combined effects of the Hall current, the nonlinear Rosseland thermal radiation, the permeability of the porous medium, and the convective heating at the surface in the unsteady three-dimensional flow of a Casson fluid along a stretching surface are investigated numerically using the spectral quasi-linearization method (SQLM). The crucial findings of the study are:

1. The effect of Lorentz force in the flow field is to resist the fluid flow in the x-direction, whereas the fluid velocity in z-direction increases near the surface, and then decreases away from the surface, within the boundary layer region. The temperature of the fluid experiences an enhancement with the increase in the strength of Lorentz force.

2. The effect of Hall current arising in the flow field is to the accelerate the fluid velocities in both the directions. The skin-friction coefficient in the x-direction decreases while the skin-friction coefficient in the z-direction increases with increasing Hall current. The Hall current tends to reduce the temperature of the fluid within the boundary layer region, which results in an increase in the rate of heat transfer at the surface.

3. Fluid velocities in both the directions increase with increasing permeability of the medium. The skin-friction coefficient in the x-direction decreases with increased permeability of the medium, whereas the skin-friction coefficient in z-direction increases with the increase in the permeability. The rate of heat transfer at the surface is higher in mediums with higher permeability. This increase in the rate of heat transfer contributes in enhancing the fluid temperature.

4. The convective heating from the surface and thermal radiation tend to raise the fluid temperature within the boundary layer region, and as a result, an increment in the heat transfer rate may also be observed.

ACKNOWLEDGMENTS

The authors are profoundly thankful to the reviewers for their valuable comments and suggestions. One of the authors, R. Nandkeolyar, is grateful to Science & Engineering Research Board, Department of Science and Technology, Government of India for providing financial assistance vide File No. ECR/2017/000118.

REFERENCES

Ashraf, M.B., Hayat, T., and Alsaedi, A., Mixed Convection Flow of Casson Fluid over a Stretching Sheet with Convective Boundary Conditions and Hall Effect, *Boundary Value Prob.*, vol. **2017**, Article ID 137, 2017.

Aziz, M.A.E., Radiation Effect on the Flow and Heat Transfer over an Unsteady Stretching Sheet, *Int. Commun. Heat Mass Transf.*, vol. **36**, pp. 521–524, 2009.

Butt, A.S., Tufaila, M.N., and Alia, A., Three-Dimensinal Flow of a Magnetohydrodynamic Casson Fluid over an Unsteady Stretching Sheet Embedded into a Porous Medium, *J. Appl. Mech. Tech. Phys.*, vol. **57**, pp. 283–292, 2016.

Chamkha, A.J., MHD-Free Convection from a Vertical Plate Embedded in a Thermally Stratified Porous Medium with Hall Effects, *Appl. Math. Modell.*, vol. **21**, pp. 603–609, 1997.

Crane, L.J., Flow past a Stretching Plate, *Z. Angew. Math. Phys.*, vol. **21**, pp. 645–647, 1970.

Elbashbeshy, E.M.A., Heat Transfer over a Stretching Surface with Variable Surface Heat Flux, *J. Phys. D: Appl. Phys.*, vol. **31**, pp. 1951–1954, 1998.

Elbashbeshy, E.M.A. and Bazid, M.A.A., Heat Transfer over an Unsteady Stretching Surface, *Heat Mass Transf.*, vol. **41**, pp. 1–4, 2004.

Eldabe, N.T.M. and Salwa, M.G.E., Heat Transfer of MHD Non-Newtonian Casson Fluid Flow between Two Rotating Cylinders, *J. Phys. Soc. Jpn.*, vol. **64**, pp. 41–64, 1995.

EL-Kabeir, S.M.M., Modather, M., and Rashad, A.M., Effect of Thermal Radiation on Mixed Convection Flow of a Nanofluid about a Solid Sphere in a Saturated Porous Medium under Convective Boundary Condition, *J. Porous Media*, vol. **18**, no. 6, pp. 569–584, 2015.

El-Kabeir, S.M.M., El-Zahar, E.R., and Rashad, A.M., Effect of Chemical Reaction on Heat and Mass Transfer by Mixed Convection Flow of Casson Fluid about a Sphere with Partial Slip, *J. Comput. Theor. Nanosci.*, vol. **13**, no. 8, pp. 5218–5226, 2016.

Gupta, A.S., Hydromagnetic Flow past a Porous Flat Plate with Hall Effects, *Acta Mech.*, vol. **22**, pp. 281–287, 1975.

Hayat, T., Abbas, Z., and Asghar, S., Effects of Hall Current and Heat Transfer on Rotating Flow of a Second Grade Fluid through a Porous Medium, *Commun. Nonlinear Sci. Numer. Simul.*, vol. **13**, pp. 2177–2192, 2008.

Hussain, S.M., Jain, J., Seth, G.S., and Rashidi, M.M., Free Convective Heat Transfer with Hall Effects, Heat Absorption and Chemical Reaction over an Accelerated Moving Plate in a Rotating System, *J. Magn. Magn. Mater.*, vol. **422**, pp. 112–123, 2017.

Ishak, A., Nazar, R., and Pop, I., Boundary Layer Flow and Heat Transfer over an Unsteady Stretching Vertical Surface, *Meccanica*, vol. **44**, pp. 369–375, 2009.

Joshi, V.K., Ram, P., Sharma, R.K., and Tripathi, D., Porosity Effect on Boundary Layer Bodewadt Flow of Magnetic Nanofluid in Presence of Geothermal Viscosity, *Eur. Phy. J. Plus*, vol. **132**, Article ID 254, 2017.

Joshi, V.K., Ram, P., Tripathi, D., and Sharma, K., Numerical Investigation of Magnetic Nanofluids Flow over Rotating Disk Embedded in a Porous Medium, *Therm. Sci.*, vol. **22**, no. 6B, pp. 2883–2895, 2018.

Khan, M.I., Waqas, M., Hayat, T., and Alsaedi, A., A Comparative Study of Casson Fluid with Homogeneous-Heterogeneous Reactions, *J. Coll. Int. Sci.*, vol. **498**, pp. 85–90, 2017.

Kumaran, V., Banerjee, A.K., Kumar, A.V., and Vajravelu, K., MHD Flow past a Stretching Permeable Sheet, *Appl. Math. Comput.*, vol. **210**, pp. 26–32, 2009.

Mahapatra, T.R. and Gupta, A.S., Heat Transfer in Stagnation-Point Flow towards a Stretching Sheet, *Heat Mass Transf.*, vol. **38**, pp. 517–521, 2002.

Makinde, O.D., Khan, Z.H., Ahmad, R., and Khan, W.A., Numerical Study of Unsteady Hydromagnetic Radiating Fluid Flow past a Slippery Stretching Sheet Embedded in a Porous Medium, *Phys. Fluids*, vol. **30**, Article ID 083601, 2018.

Mallikarjuna, B., Rashad, A.M., Hussein, A.K., and Raju, S.H., Transpiration and Thermophoresis Effects on Non-Darcy Convective Flow past a Rotating Cone with Thermal Radiation, *Arab. J. Sci. Eng.*, vol. **41**, pp. 4691–4700, 2016.

Mukhopadhyay, S., Casson Fluid Flow and Heat Transfer over a Nonlinearly Stretching Surface, *Chinese Phys.*, vol. **27**, pp. 074701–074705, 2013.

Mukhopadhyay, S. and Vajravelu, K., Diffusion of Chemically Reactive Species in Casson Fluid Flow over an Unsteady Permeable Stretching Surface, *J. Hydrodyn.*, vol. **25**, pp. 591–598, 2013.

Nabwey, H.A., El-Kabeir, S.M.M., and Rashad, A.M., Lie Group Analysis of Effects of Radiation and Chemical Reaction on Heat and Mass Transfer by Unsteady Slip Flow from a Non-Isothermal Stretching Sheet Immersed in a Porous Medium, *J. Comput. Theor. Nanosci.*, vol. **12**, pp. 4056–4062, 2015.

Nandkeolyar, R., Kameswaran, P.K., Shaw, S., and Sibanda, P., Heat Transfer on Nanofluid Flow with Homogeneous-Heterogeneous Reactions and Internal Heat Generation, *J. Heat Transf.*, vol. **136**, no. 12, Article ID 122001, 2014.

Nandkeolyar, R., Motsa, S.S., and Sibanda, P., Viscous and Joule Heating in the Stagnation Point Nanofluid Flow through a Stretching Sheet with Homogenous-Heterogeneous Reactions and Nonlinear Convection, *J. Nanotechnol. Eng. Med.*, vol. **4**, no. 4, Article ID 041002, 2013.

Nandy, S.K., Analytical Solution of MHD Stagnation-Point Flow and Heat Transfer of Casson Fluid over a Stretching Sheet with Partial Slip, *ISRN Thermodyn.*, vol. **2013**, Article ID 108264, 2013.

Pal, D., Hall Current and MHD Effects on Heat Transfer over an Unsteady Stretching Permeable Surface with Thermal Radiation, *Comput. Math. Appl.*, vol. **66**, pp. 1161–1180, 2013.

Patil, P.M., Roy, S., and Chamkha, A.J., Mixed Convection Flow over a Vertical Power-Law Stretching Sheet, *Int. J. Numer. Methods Heat Fluid Flow*, vol. **20**, no. 4, pp. 445–458, 2010.

Pavlov, K.B., Magnetohydrodynamic Flow of an Incompressible Viscous Fluid Caused by Deformation of a Surface, *Magn. Gidrodin*, vol. **4**, pp. 146–147, 1974.

Prasad, K.V., Vajravelu, K., and Vaidya, H., Hall Effect on MHD Flow and Heat Transfer over a Stretching Sheet with Variable Thickness, *Int. J. Comp. Meth. Eng. Sci. Mech.*, vol. **17**, no. 4, pp. 288–297, 2016.

Ram, P., Singh, A., and Singh, H., Effect of Porosity on Unsteady MHD Flow past a Semi-Infinite Moving Vertical Plate with Time Dependent Suction, *Ind. J. Pure Appl. Phys.*, vol. **51**, pp. 461–470, 2013.

Ram, P., Singh, H., Kumar, R., Kumar, V., and Joshi, V.K., Free Convective Boundary Layer Flow of Radiating and Reacting MHD Fluid past a Cosinusoidally Fluctuating Heated Plate, *Int. J. Appl. Comput. Math.*, vol. **3**, pp. 261–294, 2017.

Rashad, A.M., Ahmed, S.E., and Mansour, M.A., Effects of Chemical Reaction and Thermal Radiation on Unsteady Double Diffusive Convection, *Int. J. Num. Meth. Heat Fluid Flow*, vol. **24**, no. 5, pp. 1124–1140, 2014.

Rashidi, M.M., Abelman, S., and Mehr, N.F., Entropy Generation in Steady MHD Flow due to a Rotating Porous Disk in a Nanofluid, *Int. J. Heat Mass Transf.*, vol. **62**, pp. 515–525, 2013.

Reddy, N.B. and Bathaiah, D., Hall Effects on MHD Flow through a Porous Straight Channel, *Def. Sci. J.*, vol. **32**, no. 4, pp. 312–326, 1982.

Saleem, A.M. and Aziz, M.A.E., Effect of Hall Currents and Chemical Reaction on Hydromagnetic Flow of a Stretching Vertical Surface with Internal Heat Generation/Absorption, *Appl. Math. Model*, vol. **32**, pp. 1236–1254, 2008.

Sarkar, B.C., Das, S., and Jana, R.N., Hall Effects on MHD Flow in a Rotating Channel in the Presence of an Inclined Magnetic Field, *Tamkang J. Sci. Eng.*, vol. **17**, no. 3, pp. 243–252, 2014.

Sekhar, K.R., Reddy, G.V., Raju, C.S.K., Ibrahim, S.M., and Makinde, O.D., Multiple Slip Effects on Magnetohydrodynamic Boundary Layer Flow over a Stretching Sheet Embedded in a Porous Medium with Radiation and Joule Heating, *Spec. Topics Rev. Porous Media: Int. J.*, vol. **9**, no. 2, pp. 117–132, 2018.

Seth, G.S., Nandkeolyar, R., and Ansari, M.S., Hartmann Flow in a Rotating System in the Presence of Inclined Magnetic Field with Hall Effects, *Tamkang J. Sci. Eng.*, vol. **13**, no. 3, pp. 243–252, 2010.

Seth, G.S., Sharma, R., and Sarkar, S., Natural Convection Heat and Mass Transfer Flow with Hall Current, Rotation, Radiation and Heat Absorption past an Accelerated Moving Vertical Plate with Ramped Temperature, *J. Appl. Fluid Mech.*, vol. **8**, no. 1, pp. 7–20, 2015.

Seth, G.S., Tripathi, R., and Sharma, R., An Analysis of MHD Natural Convection Heat and Mass Transfer Flow with Hall Effects of a Heat Absorbing, Radiating and Rotating Fluid over an Exponentially Accelerated Moving Vertical Plate with Ramped Temperature, *Bul. Chem. Commun.*, vol. **48**, no. 4, pp. 770–778, 2016.

Shehzad, S.A., Hayat, T., Qasim, M., and Asghar, S., Effects of Mass Transfer on MHD Flow of a Casson Fluid with Chemical Reaction and Suction, *Braz. J. Chem. Eng.*, vol. **30**, pp. 187–195, 2013.

Sheikholeslami, M. and Abelman, S., Numerical Study of the Effect of Magnetic Field on Fe_3O_4-Water Ferrofluid Convection with Thermal Radiation, *Eng. Comput.*, vol. **35**, no. 5, pp. 1855–1872, 2018.

Sheikholeslami, M., Vajravelu, K., and Rashidi, M.M., Forced Convection Heat Transfer in a Semi Annulus under the Influence of a Variable Magnetic Field, *Int. J. Heat Mass Transf.*, vol. **92**, pp. 339–348, 2016.

Singh, H., Ram, P., and Kumar, V., Unsteady MHD Free Convection Fluctuating Flow past an Impulsively Started Isothermal Vertical Plate with Radiation and Viscous Dissipation, *Fluid Dyn. Mat. Proc.*, vol. **10**, no. 4, pp. 1–30, 2014.

Tufail, M.N., Butt, A.S., and Ali, A., Heat Source/Sink Effects on Non-Newtonian MHD Fluid Flow and Heat Transfer over a Permeable Stretching Surface: Lie Group Analysis, *Indian J. Phys.*, vol. **88**, pp. 75–82, 2013.

Vajravelu, K., Mukhopadhyay, S., and Gorder, R.A.V., Casson Fluid Flow and Heat Transfer at an Exponentially Stretching Permeable Surface, *J. Appl. Mech.*, vol. **80**, pp. 054502–054509, 2013.

Wang, C.Y., Liquid Film on an Unsteady Stretching Surface, *Quart. Appl. Math.*, vol. **48**, pp. 1234–1237, 1990.